How to save a bad element with weak boundary conditions

Emmanuel Hanert [a,b] and Vincent Legat [b]

[a] *Institut d'Astronomie et de Géophysique G. Lemaître, Université Catholique de Louvain, 2 Chemin du Cyclotron, B-1348 Louvain-la-Neuve, Belgium*

[b] *Centre for Systems Engineering and Applied Mechanics, Université Catholique de Louvain, 4 Avenue Georges Lemaître, B-1348 Louvain-la-Neuve, Belgium*

Abstract

The $P_1 - P_1$ finite element pair is known to allow the existence of spurious pressure (surface elevation) modes for the shallow water equations and to be unstable for mixed formulations. We show that this behavior is strongly influenced by the strong or the weak enforcement of the impermeability boundary conditions. A numerical analysis of the Stommel model is performed for both $P_1 - P_1$ and $P_1^{NC} - P_1$ mixed formulations. Steady and transient test cases are considered. We observe that the $P_1 - P_1$ element exhibits stable discrete solutions with weak boundary conditions or with fully unstructured meshes.

Key words: Shallow water equations, Stommel model, finite elements, boundary conditions, spurious elevation modes.

1 Introduction

Nowadays, an increasing interest is being paid on the use of finite element schemes in ocean modeling. Those schemes allow the use of unstructured grids which have proved to be particularly well suited to oceanic flows.

However, some finite element ocean models are known to give rise to noisy solutions when solving equations in their primitive form (e.g. Walters and Carey, 1983; Westerink et al., 1994). This is particularly the case with equal order interpolations for velocity and elevation. Different strategies have been suggested

[1] *E-mail addresses:* hanert@astr.ucl.ac.be (E. Hanert), vl@mema.ucl.ac.be (V. Legat).

to build numerical schemes that work well: mixed-order finite element interpolations (Walters, 1983), equal order elements with variables carried at set of points staggered in space (Hua and Thomasset, 1984), vorticity-divergence formulations (Staniforth and Mitchell, 1977), wave equation formulations (Lynch and Gray, 1979) and Galerkin least-squares formulations (Danilov et al., 2004).

The simplest geophysical flow model able to represent a wind-driven circulation in a closed basin with a western boundary layer is the Stommel (1948) model. It describes an incompressible, free surface flow in which the vertical pressure is hydrostatic and dissipation is linear. The model equations therefore correspond to the shallow water equations with the addition of linear friction and wind stress. The solution variables are velocity $\mathbf{u}$ and surface elevation η (equivalent to a pressure). Even if all inertial and viscous terms are neglected, such a model in its steady state requires to find a divergence free velocity field satisfying the momentum equations. In that case, the elevation plays the role of a Lagrange multiplier. An inf-sup condition should thus be satisfied between the finite element spaces for velocity and elevation to have a stable and convergent Galerkin approximation. It is not a Stokes problem but it exhibits similar numerical difficulties.

Even if some theoretical work is available on numerical models of the shallow water equations (Le Roux et al., 1998, 2004), the issue of determining suitable pairs of mixed interpolations is more known for the Stokes problem. Let us just recall that the success of a finite element model of the Stokes problem is strongly dependent upon the particular pair of velocity and pressure interpolations employed. In many cases, seemingly natural combinations produce violently oscillating pressures (Taylor and Hood, 1973; Hood and Taylor, 1974). The mathematical framework for understanding the behavior of mixed methods for the Stokes problem has been provided by Babuška (1971) and Brezzi (1974). The key requirement for a finite element scheme to work resides in the satisfaction of a stability condition, the so-called BB condition, which gives a compatibility criteria between discrete spaces. The constraints imposed by that condition are rather abstract but can usually be viewed as: (1) the number of pressure unknowns should be smaller than the number of velocity unknowns and (2) spurious pressure modes should be absent. Those criteria lead to reject the $P_1 - P_1$ finite element pair whereas other pairs, like $P_2 - P_1$, are known to work well.

For the shallow water problem, the BB condition does not strictly apply as it is designed for the Stokes problem. However, another inf-sup condition on the discrete velocity and elevation spaces exists. This condition is not strictly equivalent to the BB condition as the mathematical properties of the Coriolis operator are different from those of the usual elliptic viscous term. For instance, the Coriolis operator is a non dissipative term, whereas the viscous operator exhibits the usual smoothing property of all diffusive terms. The non

satisfaction of the discrete inf-sup condition associated to the shallow water problem is linked to the existence of spurious modes and leads to reject the $P_1 - P_1$ pair whereas $P_1^{NC} - P_1$ (Le Roux et al., 2004) or RT_0 (Miglio et al., 1999; Hanert et al., 2003) finite elements are known to work well.

In the present study, we use the Stommel model to show that finite element pairs, like $P_1 - P_1$, which are usually discarded due to spurious elevation modes can work when enforcing boundary conditions weakly rather than strongly and when using fully unstructured meshes.

2 Governing equations and mixed formulation

Let Ω be the model domain with boundary $\partial\Omega$, we seek the depth-averaged velocity $\mathbf{u}(\mathbf{x}, t)$ and the surface elevation $\eta(\mathbf{x}, t)$ which are solutions of the following equations:

$$\frac{\partial \mathbf{u}}{\partial t} + (f + \beta y)\mathbf{e}_z \times \mathbf{u} = -g\boldsymbol{\nabla}\eta - \gamma\mathbf{u} + \frac{\boldsymbol{\tau}^\eta}{\rho h}, \tag{1}$$

$$\frac{\partial \eta}{\partial t} + h\boldsymbol{\nabla} \cdot \mathbf{u} = 0, \tag{2}$$

where $\mathbf{x} = (x, y)$ is the spatial coordinate, h is the resting depth of the fluid which is assumed constant, f is the reference value of the Coriolis parameter, β is the reference value of the Coriolis parameter first derivative in the y-direction, $\mathbf{e}_z$ is a unit vector in the vertical direction, g is the gravitational acceleration, γ is a linear friction coefficient, ρ is the homogeneous density of the fluid, $\boldsymbol{\tau}^\eta$ is the wind stress acting on the surface of the fluid and $\boldsymbol{\nabla}$ is the two-dimensional gradient operator. Note that η plays a role similar to the one the pressure plays in the Navier-Stokes equations. Typically, it can be considered as the Lagrange multiplier associated to the incompressibility constraint in the steady-state case. Eqs. (1) and (2) are solved subject to no-normal flow ($\mathbf{u} \cdot \mathbf{n} = 0$ on $\partial\Omega$) boundary conditions. A complete derivation of the Stommel model, starting from the Navier-Stokes equations, may be found in (Pedlosky, 1996).

In the steady state case, a possible weak formulation of Eqs. (1) and (2) on Ω is the following:

Find $\mathbf{u} \in \mathcal{U}$ and $\eta \in \mathcal{H}$ such that:

$$< (f + \beta y)(\mathbf{e}_z \times \mathbf{u}) \cdot \hat{\mathbf{u}} > + g < \boldsymbol{\nabla}\eta \cdot \hat{\mathbf{u}} > + \gamma < \mathbf{u} \cdot \hat{\mathbf{u}} > - < \frac{\boldsymbol{\tau}^\eta}{\rho h} \cdot \hat{\mathbf{u}} >= 0 \quad \forall \hat{\mathbf{u}} \in \mathcal{U}, \tag{3}$$

$$-h < \mathbf{u} \cdot \boldsymbol{\nabla}\hat{\eta} >= 0 \quad \forall \hat{\eta} \in \mathcal{H}, \tag{4}$$

where $\mathcal{H}$ and $\mathcal{U}$ are suitable functional spaces and $< . >$ denotes the integral on Ω. Considering the transient case is a classical straightforward extension. In our formulation, the divergence term is integrated by parts and the resulting boundary integral removed. Therefore, a weak impermeability constraint is already incorporated in Eq. (4). In that case, the normal component of the velocity is not exactly zero, only its integral along the boundary vanishes. We have thus the opportunity to select a functional space $\mathcal{U}$ containing only functions that either satisfy the boundary conditions or not. In other words, we can decide to impose the no-normal flow constraint only in a weak way (as typically natural boundary conditions are imposed in second order problems) or in the usual strong way thanks to an additional constraint on the functional space. Following the classification introduced by Collatz (1966), it is the distinction between a so-called *interior method* (where the boundary conditions are satisfied by the elements of the functional space but not the partial differential equations) and a *mixed method* (where neither the boundary conditions nor the partial differential equations are satisfied by the elements of the functional space). Hence we define the following functional spaces:

$$\begin{aligned}
\mathcal{U}^w &= \{\mathbf{u} \in [L^2(\Omega)]^2\}, \\
\mathcal{U}^s &= \{\mathbf{u} \in [L^2(\Omega)]^2 \text{ and } \boldsymbol{\nabla} \cdot \mathbf{u} \in L^2(\Omega) \text{ such that } \mathbf{u} \cdot \mathbf{n} = 0 \text{ on } \partial\Omega\}, \\
\mathcal{H} &= \{\eta \in H^1(\Omega) \text{ such that } \ < \eta >= 0\},
\end{aligned}$$

where the superscripts w and s denote weak and strong boundary conditions respectively.

We then build the discrete solutions $\mathbf{u}^h$ and η^h. In this study, we focus on linear interpolations. We therefore consider $P_1 - P_1$ and $P_1^{NC} - P_1$ finite element approximations. Conforming (P_1) nodes are lying on the vertices of the triangulation and non-conforming (P_1^{NC}) nodes are located at mid-segments. Fig. 1 shows both shape functions. The $P_1^{NC} - P_1$ finite element pair has proved to be a very good element to solve the shallow water equations (Hua and Thomasset, 1984; Hanert et al., 2005). A chief advantage of that element is the orthogonality of non-conforming shape functions which permits to considerably reduce the computational cost of the scheme. Non-conforming interpolations are discontinuous everywhere except at mid-segments. They are thus a kind of compromise between continuous and discontinuous approximations. Such a discretization is very flexible and well suited to represent transport processes (Hanert et al., 2004).

In terms of functional spaces, we are now looking for $\mathbf{u}^h$ which belongs to $\mathcal{U}^s_{P_1}$, $\mathcal{U}^w_{P_1}$, $\mathcal{U}^s_{P_1^{NC}}$ or $\mathcal{U}^w_{P_1^{NC}}$ respectively. The elevation η^h always belong to the same space $\mathcal{H}_{P_1}$. Discrete equations are found by applying the standard Galerkin

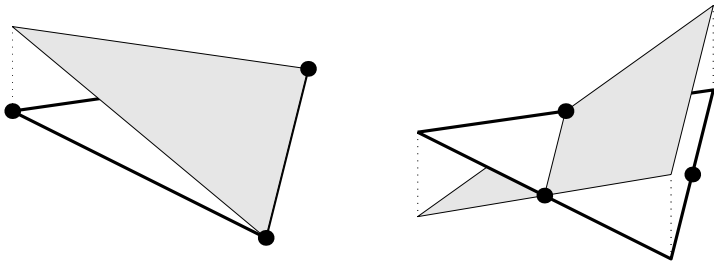

Figure 1. Linear conforming (left) and non-conforming (right) shape functions.

procedure to Eqs. (3) and (4).

For a mesh with M elements and N boundary vertices, it is usual to estimate the number of segments and vertices by $3M/2$ and $M/2$ respectively, if $M \gg N$. When the impermeability condition is strongly enforced, normal velocity degrees of freedom are constrained to zero. In that case, these variables cannot be anymore considered as degrees of freedom and, stricto sensu, the dimension of the velocity space should be decreased by the number of normal velocity nodes on the boundary ($= N$). Therefore, the finite element spaces introduced previously have approximately the following dimensions:

$$\begin{array}{ccc} \boxed{\dim(\mathcal{U}^s_{P_1}) \approx M - N} & < & \boxed{\dim(\mathcal{U}^w_{P_1}) = 2\dim(\mathcal{H}_{P_1}) \approx M} \\ \wedge & & \wedge \\ \boxed{\dim(\mathcal{U}^s_{P_1^{NC}}) \approx 3M - N} & < & \boxed{\dim(\mathcal{U}^w_{P_1^{NC}}) \approx 3M} \end{array}$$

Typically the discrete inf-sup condition associated to the steady Stommel problem requires that the size of the velocity space cannot be too small with respect to the size of the elevation space. Stability of the mixed problem increases with the size of the velocity space. However, to derive the most efficient method it is required to select the smallest velocity functional space that ensures stability (Brezzi and Fortin, 1991). To circumvent such a condition, it is possible to use a stabilized least-square Petrov-Galerkin formulation (Hughes et al., 1986) defined as follows:

Find $\mathbf{u} \in \mathcal{U}$ and $\eta \in \mathcal{H}$ such that:

$$\begin{aligned} &< (f + \beta y)(\mathbf{e}_z \times \mathbf{u}) \cdot \hat{\mathbf{u}} > + g < \boldsymbol{\nabla}\eta \cdot \hat{\mathbf{u}} > \\ &\qquad + \gamma < \mathbf{u} \cdot \hat{\mathbf{u}} > - < \frac{\boldsymbol{\tau}^\eta}{\rho h} \cdot \hat{\mathbf{u}} >= 0 \quad \forall \hat{\mathbf{u}} \in \mathcal{U}, \\ &-h < \mathbf{u} \cdot \boldsymbol{\nabla}\hat{\eta} > + \varepsilon < (f + \beta y)(\mathbf{e}_z \times \mathbf{u}) \cdot \boldsymbol{\nabla}\hat{\eta} > + \varepsilon g < \boldsymbol{\nabla}\eta \cdot \boldsymbol{\nabla}\hat{\eta} > \end{aligned} \tag{5}$$

$$+\varepsilon\gamma < \mathbf{u}\cdot\boldsymbol{\nabla}\hat{\eta} > +\varepsilon < \frac{\boldsymbol{\tau}^{\eta}}{\rho h}\cdot\boldsymbol{\nabla}\hat{\eta} >= 0 \quad \forall\hat{\eta}\in\mathcal{H}, \tag{6}$$

where the coefficient ε fixes the importance of the stabilization term versus the continuity equation. That formulation permits to enhance stability without upsetting consistency. Brezzi and Douglas (1988) proved that the error introduced by the additional term is minimal under the condition that $\varepsilon = \mathcal{O}(d^2)$, where d is the element size.

3 Steady problem

We first consider the numerical resolution of the steady Stommel problem with $P_1 - P_1$ and $P_1^{NC} - P_1$ finite elements. Boundary conditions are weakly and strongly enforced. The computational domain is the interval $[0, L] \times [0, L]$ where $L = 10^6$ m. The physical parameters f, β, g, γ, ρ and h are respectively set to 10^{-4} s^{-1}, 10^{-11} m^{-1}s^{-1}, 10 m^{2}s^{-1}, 10^{-6} s^{-1}, 1000 kg m^{-3} and 1000 m. The wind field has the following expression:

$$\boldsymbol{\tau}^{\eta} = \begin{pmatrix} 0.2\sin(y - L/2) \\ 0 \end{pmatrix} \text{ kg m}^{-1}\text{s}^{-2}.$$

The values of the physical parameters are realistic in the context of ocean modeling.

An illustration of the numerical solution obtained with the $P_1^{NC} - P_1$ finite element pair when imposing weak boundary conditions in given in Fig. 2. In that case, both schemes are working well. When enforcing boundary conditions strongly, the $P_1^{NC} - P_1$ scheme is still working well whereas it is impossible to obtain a discrete solution with the $P_1 - P_1$ scheme as the discrete matrix becomes singular. For the latter scheme, a stabilized least-squares Petrov-Galerkin formulation has to be used to obtain an acceptable solution.

As there is an analytical solution to the steady Stommel problem (Mushgrave, 1985), it is possible to compute the L_2-error on the numerical solution. Fig. 3 shows the error on the elevation field when using the $P_1 - P_1$ scheme with weak boundary conditions, the stabilized $P_1 - P_1$ scheme with strong boundary conditions and the $P_1^{NC} - P_1$ scheme with strong and weak boundary conditions. The physical parameters are the same as previously. As expected, all schemes show quadratic convergence rates.

For the $P_1 - P_1$ scheme, a weak enforcement of boundary conditions is more accurate than stabilizing the scheme and imposing boundary conditions strongly.

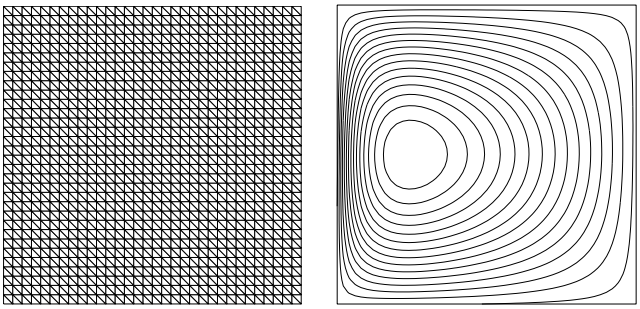

Figure 2. Steady state elevation field obtained with the $P_1^{NC} - P_1$ (right) finite element scheme. No normal flow boundary conditions are weakly imposed. The grid is structured and composed of 2048 biased right isocele triangles (left). The contour interval is 0.0048 m.

This is due to the stabilization procedure which amounts to put a consistent diffusion term in the mass equation. That term yields a coupling of neighboring elevation unknowns, and consequently has a smoothing effect. The gain of stability is thus obtained at the cost of a greater numerical error.

For the $P_1^{NC} - P_1$ scheme, it appears to be a better strategy to apply boundary conditions in the usual strong way. As we have approximately six times more velocity nodal values than elevation nodal values, the scheme is stable with strong and weak boundary conditions. Therefore, enforcing boundary conditions strongly decreases the ratio between the number of velocity and elevation degrees of freedom. This ratio then goes toward the optimal value, just on the edge of stability. In simple words, this results in a decrease of the stability and an increase of the accuracy of the numerical solution. As we have more velocity degrees of freedom with the $P_1^{NC} - P_1$ element than with the $P_1 - P_1$ element, we always observe a better accuracy with the former when using the same mesh. On the other hand, the opposite conclusion is observed when both schemes have the same number of degrees of freedom.

As for the Stokes problem, the violation of a discrete inf-sup condition is associated with the existence of spurious elevation (pressure) modes. These modes are non constant eigenvectors lying in the null space of the discrete gradient operator. They are thus such that $\mathbf{u} = 0$ and $\boldsymbol{\nabla}\eta = 0$ for non trivial η (Walters and Carey, 1983, 1984). For elements not respecting the discrete inf-sup condition, a zero discrete elevation gradient does not guarantee that the discrete elevation is constant. Solution uniqueness is lost as any multiple of a spurious mode can be added to any solution of the discrete equations and still satisfy them.

The existence of spurious elevation modes can be assessed by computing the dimension of the null space of the discrete gradient operator. Such an analysis has been performed by Le Roux et al. (2004) for various finite element pairs but only with strong boundary conditions and uniform grids. Following the

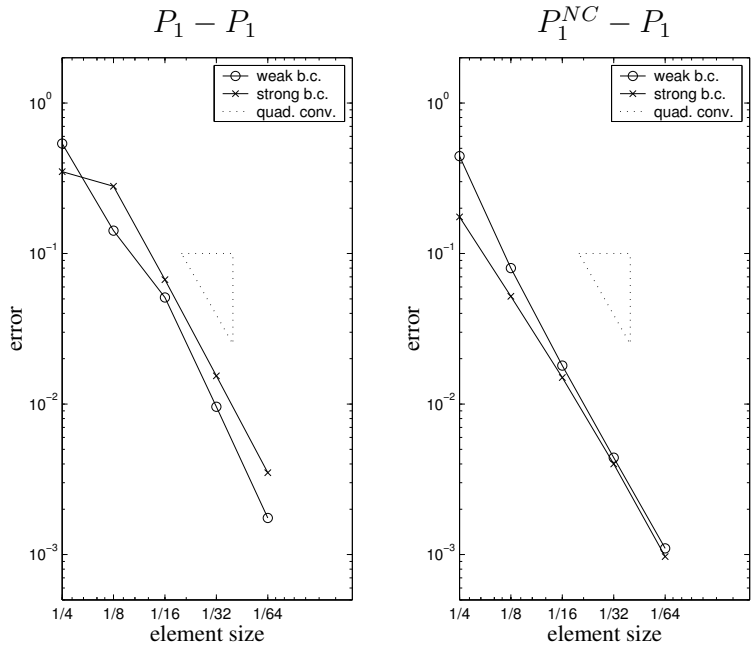

Figure 3. L_2-error on the elevation field with different uniform meshes for the $P_1 - P_1$ (left) and $P_1^{NC} - P_1$ (right) finite element schemes with strong ($\times$) and weak ($\circ$) boundary conditions. The convergence rate is quadratic in each case.

same approach, we present results for the $P_1 - P_1$ and $P_1^{NC} - P_1$ schemes with strong and weak boundary conditions in Fig. 4. It is particularly interesting to note the discrepancy in observations for structured-uniform, structured-distorted and unstructured meshes.

Among the schemes examined, only the $P_1 - P_1$ finite element pair with strong boundary conditions can exhibit spurious elevation modes. For uniform and distorted structured meshes, the dimension of the null space of the discrete gradient operator is greater than one. This observation is independent of the size of the mesh. It is interesting to note that when using an unstructured mesh, spurious elevation modes are absent and, one is able to obtain a discrete solution. For all the other finite element schemes, we have one eigenvector, the hydrostatic mode, which can be simply considered as the undetermined constant elevation associated with the resolution of the governing equations.

4 Transient problem

When solving the transient equations, the continuity equation is no longer a constraint on the velocity field but a prognostic equation for the elevation. As a result, it is not clear that a discrete inf-sup condition applies. However, spurious elevation modes are still an issue and the selected finite element

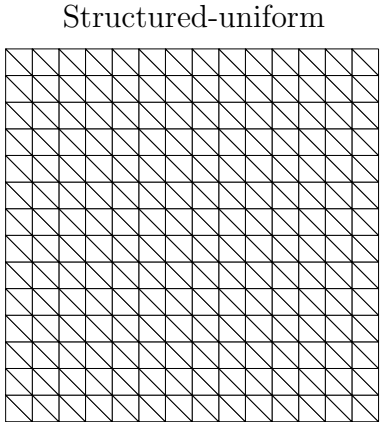

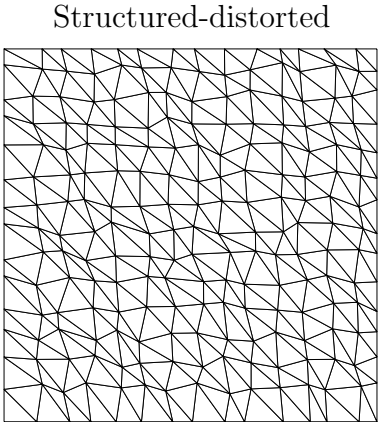

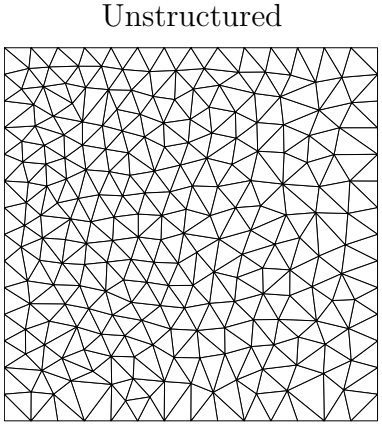

	$P_1 - P_1$	$P_1^{NC} - P_1$
strong	4	1
weak	1	1

	$P_1 - P_1$	$P_1^{NC} - P_1$
strong	3	1
weak	1	1

	$P_1 - P_1$	$P_1^{NC} - P_1$
strong	1	1
weak	1	1

Figure 4. Dimension the discrete gradient null space for the $P_1 - P_1$ and $P_1^{NC} - P_1$ finite element schemes when using strong and weak boundary conditions.

scheme should not allow their existence.

As an illustration of a transient problem, we consider the propagation of slow Rossby modes. The particular case of an equatorial Rossby soliton (Boyd, 1980) is examined. Rossby waves are slow propagating waves that play an important role in geophysical flows as they carry a significant amount of energy. Equatorial Rossby soliton are Rossby waves confined to a narrow band about the equator by the Coriolis force. To accurately represent those waves, a nonlinear model should be used. However, in the present experiment, we only want to assess the different numerical models and see if they allow the existence of spurious elevation modes. For the sake of simplicity, we therefore consider a linear model.

The simulations are run as reduced gravity models with parameters set to correspond to the first internal vertical mode of a baroclinic model. There is no bottom drag and wind forcing. The reduced gravity, mean depth and Coriolis parameters are taken as $g' = 4 \times 10^{-2}$ ms^{-2}, $h = 100$ m, $f = 0$ s^{-1} and $\beta = 10^{-11}$ m^{-1}s^{-1} respectively. Those values yield a time scale (T) of 41 h, a length scale (L) of 296 km and a velocity scale (U) of 2 ms^{-1}. The scaling factors are defined as

$$L = \frac{a}{E^{1/4}}, \quad T = \frac{E^{1/4}}{2\Omega}, \quad U = \sqrt{g'h},$$

where E is the so-called Lamb parameter (Boyd, 1980) defined as $E = 4\Omega^2 a^2/(g'h)$.

The parameters $a = 6.3 \times 10^6$ m and $\Omega = 7.27 \times 10^{-5}$ s^{-1} respectively denote the radius of the Earth and the angular frequency of the Earth rotation.

The rectangular domain extent is $32L \times 8L$. Simulations are performed on structured-uniform and unstructured meshes (Fig. 5a). In each case, the element size is approximately $L/3$. The same initial conditions as those introduced by Boyd (1980) are prescribed (Fig. 5b). The model equations are discretized in time with a second-order, centered in time, Crank-Nicolson implicit scheme. The time step is set to $T/4$.

At the beginning of the integration, the soliton loses approximately 5% of its amplitude which propagates eastward as an equatorial Kelvin wave. This is due to the initial condition that is not exactly a solitary wave. Meanwhile, the soliton propagates westward at approximately the same speed for all numerical schemes. The amplitude of the soliton decreases during propagation because nonlinear terms have been neglected. With a nonlinear model, the amplitude would stay almost constant during propagation. The elevation fields obtained after 32 nondimensional time units when using structured and unstructrured meshes are shown in Fig. 6 and Fig. 7 respectively. We consider $P_1 - P_1$ and $P_1^{NC} - P_1$ finite elements with strong and weak boundary conditions as well as stabilized $P_1 - P_1$ finite elements with strong boundary conditions.

On a structured mesh, the $P_1 - P_1$ scheme with strong boundary conditions is the only to produce a solution polluted by spurious oscillations. A stabilization is therefore required to obtain an acceptable solution. Other schemes, including $P_1 - P_1$ with weak boundary conditions, give good results. When using an unstructured mesh, even the $P_1 - P_1$ scheme with strong boundary conditions does not exhibit spurious oscillations. In that case, all schemes work well without stabilization procedures. Such a change in the numerical behavior when going from a structured to an unstructured mesh is due to the null space of the discrete gradient operator. As shown previously, the dimension of the latter is greater than one in the structured case and equal to one in the unstructured case.

As shown in Fig. 8, a weak imposition of boundary conditions does not assure that the normal component of the velocity field is zero on each boundary node. We present a close-up view of the velocity field in the soliton, just above the lower boundary. The $P_1 - P_1$ finite element scheme has been used with weak and strong boundary conditions. As expected, the normal velocity on the boundary is not exactly zero while the impermeability constraint is weakly enforced. This might be a problem if an accurate representation of the flow on the boundaries is required. However in oceanic or coastal flows, the position of the boundaries is not precisely known as the coastline has a fractal geometry. Moreover, the separation between land and sea may change in time due to flooding and drying processes. Therefore, a weak imposition

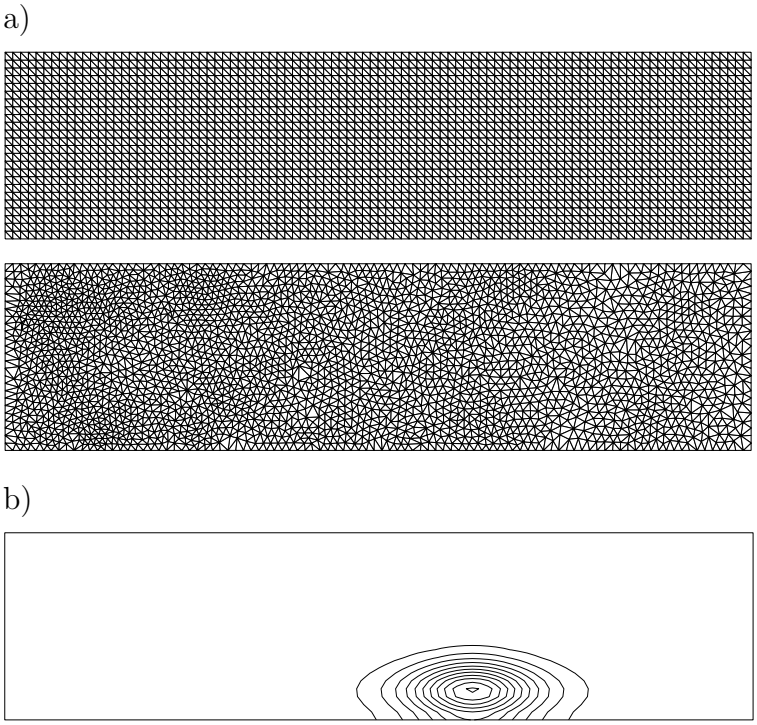

Figure 5. (a) Structured and unstructured meshes used in the equatorial Rossby soliton experiment. (b) Isolines of the elevation field at initial time. The contour interval is 0.0154 m.

of boundary conditions is justified for such applications. It should also be pointed out that, on a curved domain, when the velocity field is approximated with P_1 shape functions, the impermeability constraint is also approximatively satisfied. Indeed, in that case velocity nodes are lying on the vertices and it is not possible to define a normal vector on these nodes in a unique way.

5 Conclusions

When solving the shallow water equations, the way to impose the impermeability boundary condition has a crucial impact on the numerical solution. Indeed, some finite element pairs, like $P_1 - P_1$, which are usually discarded due to spurious elevation modes, work well when boundary conditions are weakly enforced. In that case, spurious elevation modes are absent. On the other hand, for finite element pairs like $P_1^{NC} - P_1$, where there are much more velocity than elevation nodes, better results are obtained with strong boundary conditions.

Finally, we have to emphasize that we neglect viscous and transport terms in the simplified model. It is not straightforward to directly extrapolate our conclusions to the full non-linear model. However, such an extrapolation is

$P_1 - P_1$ strong

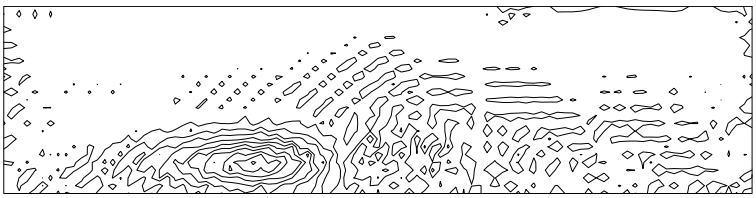

$P_1 - P_1$ strong stabilized

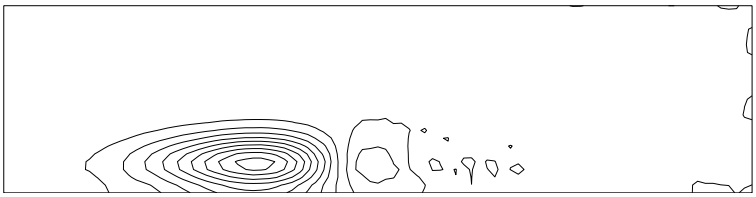

$P_1 - P_1$ weak

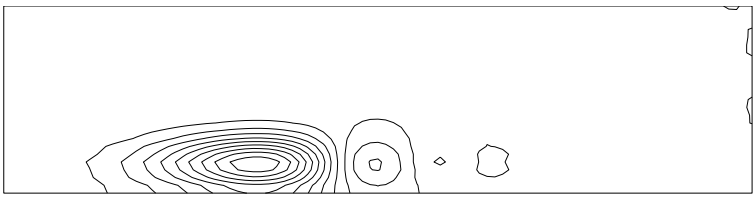

$P_1^{NC} - P_1$ strong

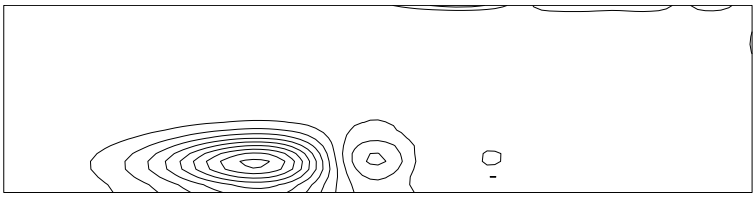

$P_1^{NC} - P_1$ weak

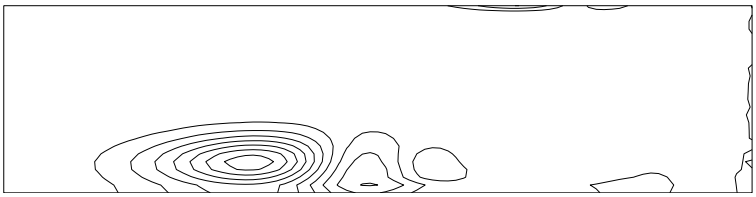

Figure 6. Elevation field after 55 days ($32T$) for the $P_1 - P_1$ and $P_1^{NC} - P_1$ finite element schemes when using strong and weak boundary conditions. The contour interval is the same as in Fig. 5. The mesh is structured uniform.

$P_1 - P_1$ strong

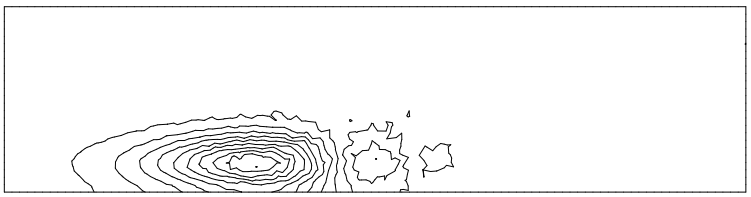

$P_1 - P_1$ strong stabilized

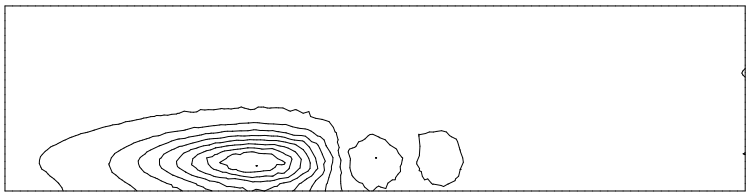

$P_1 - P_1$ weak

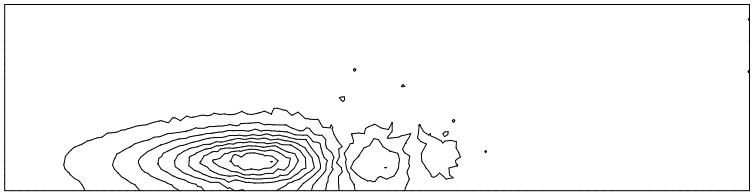

$P_1^{NC} - P_1$ strong

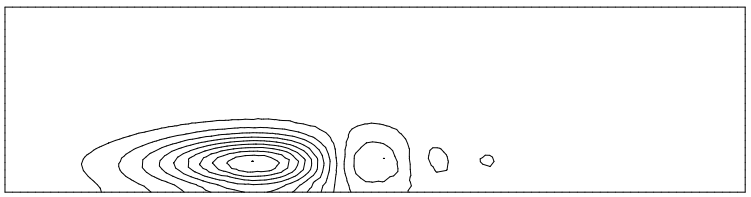

$P_1^{NC} - P_1$ weak

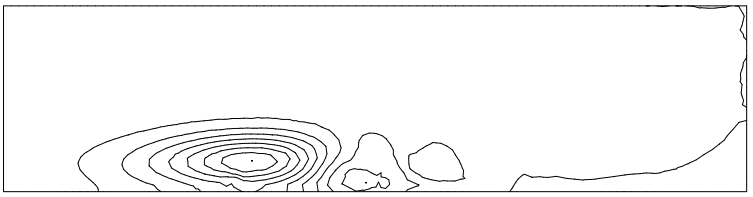

Figure 7. Same as Fig. 6 except that the mesh is unstructured.

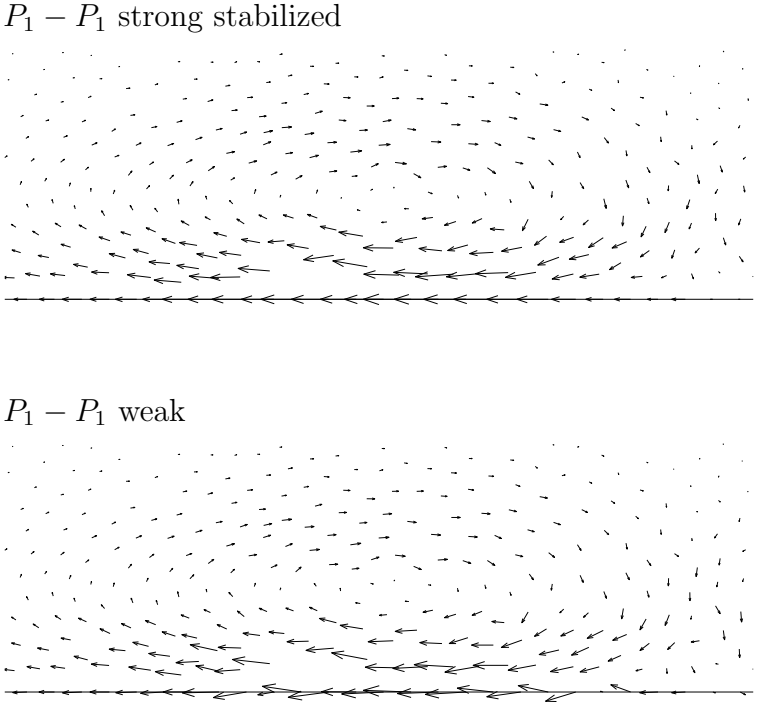

Figure 8. Close-up view of the velocity field after 55 days ($32T$) in the soliton, just above the lower boundary. Solutions are obtained with the $P_1 - P_1$ finite element scheme using strong and weak boundary conditions. The mesh is unstructured.

often used for the Navier-Stokes equations to apply theoretical results valid for the Stokes problem. Therefore, we expect that the same numerical observations appear for the Stokes problem. Indeed, the $P_1 - P_1$ finite element pair should provide a stable and convergent behaviour for Navier-Stokes equations when the boundary conditions are applied in a suitable weak form. The last open question is how is it possible to implement weak Dirichlet boundary conditions for Navier-Stokes equations without deteriorating the global accuracy.

Acknowledgements

Emmanuel Hanert is Postdoctoral Researcher with the Belgian National Fund for Scientific Research (FNRS). The curiosity and the help of Adrien Leygue and all the students registrated in 2003-2004 to the UCL-course MECA2120 "Introduction to Finite Elements" is gratefully acknowledged. The present study was carried out within the scope of the project "A second-generation model of the ocean system", which is funded by the *Communauté Française de Belgique*, as *Actions de Recherche Concertées*, under the contract ARC 04/09-316. This work is a contribution to the development of SLIM, the Second-generation Louvain-la-neuve Ice-ocean Model.

References

Babuška, I., 1971. Error bounds for finite element methods. Numerische Mathematik 16, 322–333.

Boyd, J.P., 1980. Equatorial solitary waves. Part I: Rossby solitons. Journal of Physical Oceanography 10, 1699–1717.

Brezzi, F., 1974. On the existence, uniqueness and approximation of saddle point problems arising from Lagrangian multipliers. R.A.I.R.O. Analyse Numérique 8, 129–151.

Brezzi, F., Douglas, J., 1988. Stabilized mixed methods for the Stokes problem. Numerische Mathematik 53, 225–235.

Brezzi, F., Fortin, M., 1991. Mixed and Hybrid Finite Element Methods. No. 15 in Springer Series in Computational Mathematics. Springer-Verlag.

Collatz, L., 1966. The Numerical Treatment of Differential Equations. Springer-Verlag.

Danilov, S., Kivman, G., Schröter, J., 2004. A finite element ocean model: Principles and evaluation. Ocean Modelling 6, 125–150.

Hanert, E., Le Roux, D.Y., Legat, V., Deleersnijder, E., 2004. Advection schemes for unstructured grid ocean modelling. Ocean Modelling 7, 39–58.

Hanert, E., Le Roux, D.Y., Legat, V., Deleersnijder, E., 2005. An efficient Eulerian finite element method for the shallow water equations. Ocean Modelling, in press.

Hanert, E., Legat, V., Deleersnijder, E., 2003. A comparison of three finite elements to solve the linear shallow water equations. Ocean Modelling 5, 17–35.

Hood, P., Taylor, C., 1974. Navier-Stokes equations using mixed interpolations. In: Oden, J.T., Zienkiewicz, O.C., Gallagher, R.H., Taylor, C. (Eds.), Finite Element Methods in Flow Problems. University of Alabama Press, pp. 121–132.

Hua, B.L., Thomasset, F., 1984. A noise-free finite element scheme for the two-layer shallow water equations. Tellus 36A, 157–165.

Hughes, T.J.R., Franca, L.P., Balestra, M., 1986. A new finite element formulation for computational fluid dynamics: V. Circumventing the Babuška-Brezzi condition: A stable Petrov-Galerkin formulation of the stokes problem accomodating equal-order interpolations. Computer Methods in Applied Mechanics and Engineering 59, 85–99.

Le Roux, D.Y., Sene, A., Rostand, V., Hanert, E., 2004. On some spurious modes issues in shallow water models using a linear algebra approach. Ocean Modelling, in press.

Le Roux, D.Y., Staniforth, A., Lin, C.A., 1998. Finite elements for shallow-water equation ocean models. Monthly Weather Review 126:7, 1931–1951.

Lynch, D.R., Gray, W.G., 1979. A wave equation model for finite-element tidal computations. Computers and Fluids 7, 207–228.

Miglio, E., Quarteroni, A., Saleri, F., 1999. Finite element approximation of quasi-3D shallow water equations. Computer Methods in Applied Mechanics

and Engineering 174, 355–369.
Mushgrave, D.L., 1985. A numerical study of the roles of subgyre-scale mixing and the western boundary current on homogeniztion of a passive tracer. Journal of Geophysical Research 90, 7037–7043.
Pedlosky, J., 1996. Ocean circulation theory. Springer-Verlag.
Staniforth, A.N., Mitchell, H., 1977. A semi-implicit finite-element barotropic model. Monthly Weather Review 105, 154–169.
Stommel, H., 1948. The westward intensification of wind-driven ocean currents. Transactions of the American Geophysical Union 29, 202–206.
Taylor, C., Hood, P., 1973. A numerical solution of the Navier-Stokes equations using FEM techniques. Computer and Fluids 1, 73–100.
Walters, R.A., 1983. Numerically induced oscillations in finite element approximations to the shallow water equations. International Journal for Numerical Methods in Fluids 3, 591–604.
Walters, R.A., Carey, G.F., 1983. Analysis of spurious oscillations modes for the shallow water and Navier-Stokes equations. Computer and Fluids 11, 51–68.
Walters, R.A., Carey, G.F., 1984. Numerical noise in ocean and estuarine models. Advances in Water Resources 7, 15–20.
Westerink, J.J., Luetich, R.A., Wu, J.K., Kolar, R.L., 1994. The influence of normal flow boundary conditions on spurious modes in finite element solutions to the shallow water equations. International Journal for Numerical Methods in Fluids 18, 1021–1060.